

UC Davis

UC Davis Previously Published Works

Title

Magnetic properties and colossal magnetoresistance of La(Ca)MnO₃ materials doped with Fe.

Permalink

<https://escholarship.org/uc/item/2wz1x8dx>

Journal

Physical review. B, Condensed matter, 54(21)

ISSN

0163-1829

Authors

Ahn, KH
Wu, XW
Liu, K
[et al.](#)

Publication Date

1996-12-01

DOI

10.1103/physrevb.54.15299

Peer reviewed

Magnetic properties and colossal magnetoresistance of La(Ca)MnO₃ materials doped with Fe

K. H. Ahn, X. W. Wu, K. Liu, and C. L. Chien

Department of Physics and Astronomy, The Johns Hopkins University, Baltimore, Maryland 21218

(Received 1 August 1996)

The effect of Fe doping (<20%) on the Mn site in the ferromagnetic ($x=0.37$) and the antiferromagnetic ($x=0.53$) phases of La_{1-x}Ca_xMnO₃ has been studied. The same ionic radii of Fe³⁺ and Mn³⁺ cause no structure change in either series, yet conduction and ferromagnetism have been consistently suppressed by Fe doping. Colossal magnetoresistance has been shifted to lower temperatures, and in some cases enhanced by Fe doping. Doping with Fe bypasses the usually dominant lattice effects, but depopulates the hopping electrons and thus weakens the double exchange. [S0163-1829(96)09545-8]

Recently, perovskite-based oxides have been the subjects of intense research efforts.¹ They exhibit a variety of transport and magnetic properties that sensitively depend on the stoichiometry and structure of the materials. Most of the attention to date has been focused on doping the parent compound of LaMnO₃ with divalent alkaline earths (e.g., Ca, Ba, Sr), such as the prototype materials of La_{1-x}Ca_xMnO₃, which exhibit a very rich phase diagram.² At low Ca doping ($x<0.2$), the materials are ferromagnetic (FM) insulators, whereas at high Ca doping ($x>0.5$), the materials become antiferromagnetic (AF) insulators. In the intermediate doping range of $0.2<x<0.5$, one observes both FM and metallic behavior, which leads to colossal magnetoresistance¹ (CMR) near the onset of FM ordering. Interestingly, in the AF insulating phase ($x\approx 0.5$), CMR with a large magnitude has also been observed.³ The observation of CMR has generated a surge of interest in these materials, which are often referred to as the CMR materials.

Double exchange⁴ (DE) has been featured prominently in the discussion of the fascinating properties of the CMR materials. Doping the insulating LaMnO₃ material, in which only Mn³⁺ exists, with the divalent ions (Ca, Ba, etc.) causes the conversion of a proportional number of Mn³⁺ to Mn⁴⁺. Because of the strong Hund's coupling, the electronic configurations are Mn³⁺($t_{2g}^3e_g^1$) and Mn⁴⁺($t_{2g}^3e_g^0$). The presence of Mn⁴⁺, due to the doping, enables the e_g electron of a Mn³⁺ ion to hop to the neighboring Mn⁴⁺ ion via DE, which mediates ferromagnetism and conduction. The DE, and consequently, the physical properties of these materials, are particularly susceptible to the lattice effects brought on by doping. Very strong lattice effects have been realized when the La ions are partially replaced by trivalent or divalent ions of *different* size. Any deviation from the ideal cubic perovskite structure can lead to either a reduction in the Mn-O-Mn bond angle from 180°, or a change in the bond length, both directly affecting the DE.

To date, much of the exploration of the CMR materials has been done through doping of the La sites, which brings about lattice effects, and ultimately influences the DE. However, far fewer studies have been conducted in doping the Mn sites, which are at the heart of the DE. In this work, we have undertaken a study of the doping of the Mn sites by Fe in La_{1-x}Ca_xMnO₃ with $x=0.37$ and $x=0.53$. The undoped starting materials of La_{0.63}Ca_{0.37}MnO₃ and La_{0.47}Ca_{0.53}MnO₃

are the FM and the AF phases, respectively, where CMR has been previously reported. Early studies have shown that in this Fe doping range, a direct replacement of Mn³⁺ by Fe³⁺ occurs.⁵ Also unique to this doping, Mn³⁺ and Fe³⁺ have *identical* ion size.⁶ Consequently, the otherwise strong lattice effects can be bypassed, and the effects due to changes in the electronic structure become accessible.

Samples were fabricated with conventional solid-state reaction methods. Stoichiometric mixtures of La₂O₃, CaCO₃, Fe₂O₃, and MnCO₃ were pressed into pellets and heated in an oxygen atmosphere for 144 h with two intermediate grindings. The temperature for the first two sinterings was 1200 °C, and 1300 °C for the last one. The chemical formula for the final compounds is La_{1-x}Ca_xMn_{1-y}Fe_yO₃, where $y<0.20$ with $x=0.37$ and $x=0.53$.

Powder x-ray diffraction shows single-phase tetragonally distorted perovskite structure for all samples. For the series of La_{0.63}Ca_{0.37}Mn_{1-y}Fe_yO₃, no appreciable difference in the diffraction patterns has been observed among the Fe-doped samples; all having the same lattice parameters of $a=b=5.45$ Å and $c=7.72$ Å. Similarly, the La_{0.47}Ca_{0.53}Mn_{1-y}Fe_yO₃ samples have the same lattice parameters of $a=b=5.42$ Å and $c=7.63$ Å. These results demonstrate the replacement of Mn by Fe without any structural change and that the lattice effects have indeed been bypassed. Our results are also in agreement with Jonker's earlier conclusion⁵ that Mn³⁺ is replaced by the same size Fe³⁺. We have employed the standard ferrous sulfate and potassium permanganate titration method⁷ to determine the Mn valence. The results show ideal stoichiometry.

The temperature dependence of the magnetization M at $H=0.01$ T and the resistivity ρ at $H=0$ (solid curves) and $H=5$ T (dashed curves) for the FM La_{0.63}Ca_{0.37}Mn_{1-y}Fe_yO₃ is shown in Figs. 1(a) and 1(b), respectively. The undoped sample undergoes a paramagnetic (PM) to FM transition at $T_c\approx 260$ K, accompanied by a simultaneous insulator-to-metal transition, consistent with the results reported previously.² As Fe is doped into the sample, both T_c and M are systematically lowered [Fig. 1(a)]. The value of T_c is suppressed to about 170 K for the sample with $y=0.08$, further lowered to 60 K for $y=0.12$, and to 40 K for $y=0.18$. The sample resistivity ρ , on the other hand, increases with Fe doping, as shown in Fig. 1(b). In every case, a peak in ρ , characteristic of a metal-insulator transition, occurs near T_c .

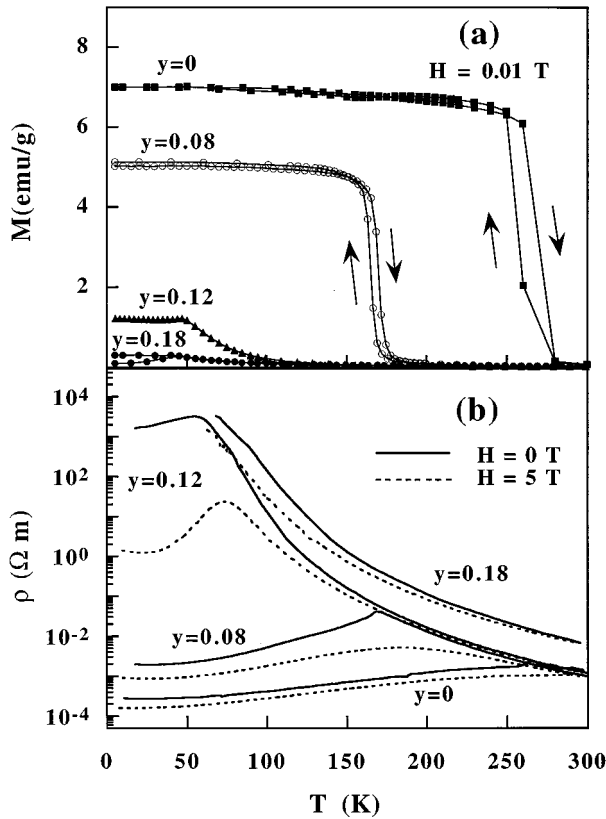


FIG. 1. Temperature dependence of (a) the magnetization M in a 0.01 T field, and (b) the resistivity ρ in zero (solid curves) and 5 T (dashed curves) magnetic field, for $\text{La}_{0.63}\text{Ca}_{0.37}\text{Mn}_{1-y}\text{Fe}_y\text{O}_3$ with $y=0, 0.08, 0.12,$ and 0.18 .

It is also noted that, upon Fe doping, the large negative magnetoresistance, or CMR, is dramatically enhanced. For the undoped sample ($y=0$), CMR of 120% is observed near T_c . For $y=0.08$, a 5 T field reduces ρ by one order of magnitude. For $y=0.12$, the CMR effect increases to three orders of magnitude. However, further doping to $y=0.18$, shows insulating behavior in the whole temperature range, with or without a 5 T field, although a sizable MR still remains.

The $\text{La}_{0.47}\text{Ca}_{0.53}\text{Mn}_{1-y}\text{Fe}_y\text{O}_3$ series, on the other hand, shows more complicated behavior in the undoped samples as well as those doped ones. The magnetization data with $H=1$ T are shown in Fig. 2(a). The undoped sample ($y=0$) first undergoes a PM to FM transition at about 250 K. As the temperature is further lowered, M begins to decrease to lower values when FM ordering reverts to AF. This is in agreement with the reported results in $\text{La}_{0.5}\text{Ca}_{0.5}\text{MnO}_3$,² where an intermediate FM state was observed between the PM state at high temperatures and the AF state at low temperatures. The intermediate transition between FM and AF is first-order in nature, accompanied by large thermal hysteresis. Upon Fe doping, the intermediate FM phase rapidly diminishes. At $y=0.09$, the FM state disappears and only the PM to AF transition at about 50 K remains. Further doping with Fe has a less effect on the PM to AF transition. It is noted that for the $y=0.09$ sample, an additional broad extremum in M at about 210 K is observed, possibly due to charge ordering.

The temperature dependence of the resistivity ρ at $H=0$

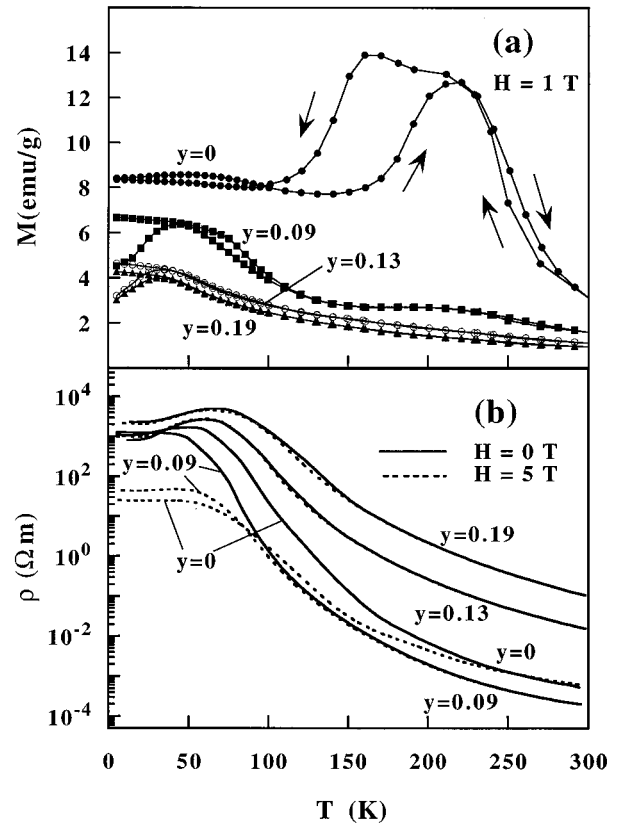


FIG. 2. Temperature dependence of (a) the magnetization M in a 1 T field, and (b) the resistivity ρ in zero (solid curves) and 5 T (dashed curves) magnetic field, for $\text{La}_{0.47}\text{Ca}_{0.53}\text{Mn}_{1-y}\text{Fe}_y\text{O}_3$ with $y=0, 0.09, 0.13,$ and 0.19 .

(solid curves) and at $H=5$ T (dashed curves) of $\text{La}_{0.47}\text{Ca}_{0.53}\text{Mn}_{1-y}\text{Fe}_y\text{O}_3$ is shown in Fig. 2(b). All samples are insulating in nature at all temperatures, even under a 5 T field, while the magnetization has a rich temperature dependence as shown in Fig. 2(a). The temperature dependence of ρ for various samples is qualitatively similar. The resistivity ρ increases with decreasing temperature, leveling off at 60 K. Although Fe doping generally increases the resistivity, the initial Fe doping ($y=0.09$) actually lowers ρ . As for the magnetoresistance, the undoped ($y=0$) and the lightly doped ($y=0.09$) samples show negative MR by as much as two orders of magnitude at low temperatures. As the doping is further increased ($y=0.13$ and $y=0.19$), there is virtually no MR.

Magnetic hysteresis loops with field up to 5 T have been measured at 5 K for all samples. The magnetizations, normalized to the value at 5 T, are shown in Fig. 3. For the $\text{La}_{0.63}\text{Ca}_{0.37}\text{Mn}_{1-y}\text{Fe}_y\text{O}_3$ series, shown in Fig. 3(a), samples with $y=0$ and $y=0.08$ show virtually the same FM behavior, each exhibiting saturation magnetization and square hysteresis loop. However, the magnetization of the samples with $y=0.12$ and $y=0.18$ cannot be saturated. The resultant magnetization curves are essentially a superposition of both the FM and AF components, indicating a canted spin state. The saturation magnetization of the FM component can be determined by extrapolating the linear part of the magnetization to $H=0$. These values displayed as saturation moment per formula unit μ_s are shown in the inset of Fig. 3(a). The dashed line in the inset represents the maximum value of μ_s when

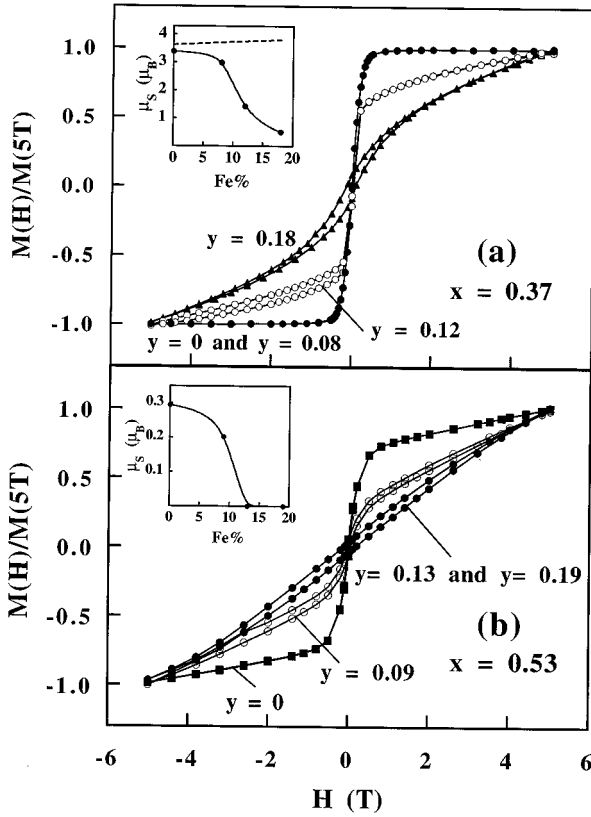


FIG. 3. Magnetic hysteresis loops measured at 5 K for $\text{La}_{1-x}\text{Ca}_x\text{Mn}_{1-y}\text{Fe}_y\text{O}_3$ with (a) $x=0.37$ and (b) $x=0.53$. The insets show the saturation magnetic moment μ_s per formula unit vs Fe content for each series. The dashed line indicates the values for full alignment of all the Mn and Fe moments.

all the Mn and Fe moments, $4.0\mu_B$ for Mn^{4+} , $5.0\mu_B$ for Mn^{3+} , and $5.9\mu_B$ for Fe^{3+} , are aligned. The measured value of μ_s is nearly that of the fully aligned moment for the $y=0$ sample, but steadily declines upon Fe doping. Clearly, the presence of Fe, instead of enhancing, actually suppresses ferromagnetism.

The $\text{La}_{0.47}\text{Ca}_{0.53}\text{Mn}_{1-y}\text{Fe}_y\text{O}_3$ samples, as shown in Fig. 3(b), do not show pure FM behavior for any composition. Canted spin AF state has already set in for the samples with $y=0$ and $y=0.09$, both showing small FM components. The determined values of μ_s are only about $0.3\mu_B$, about a factor of 10 smaller than those shown in Fig. 3(a). Upon further Fe doping, no FM component but AF behavior can be observed. From the results shown in Figs. 3(a) and 3(b), it is evident that Fe doping enhances AF ordering.

It is well known that double exchange mediates ferromagnetism and metallic conduction. The transport and magnetic results shown above clearly demonstrate that partial replacement of Mn by Fe favors insulating and AF behavior, opposing the effects of the double exchange. Since Fe doping is the direct replacement of Mn^{3+} by Fe^{3+} , the experimental results suggest that the sites that are now occupied by Fe^{3+} can no longer effectively participate in the double exchange process. The mechanism that Fe^{3+} terminates the double exchange process arises purely from the electronic structure of the materials as we describe in the following.

In perovskite oxides, the d electrons of the Mn and Fe

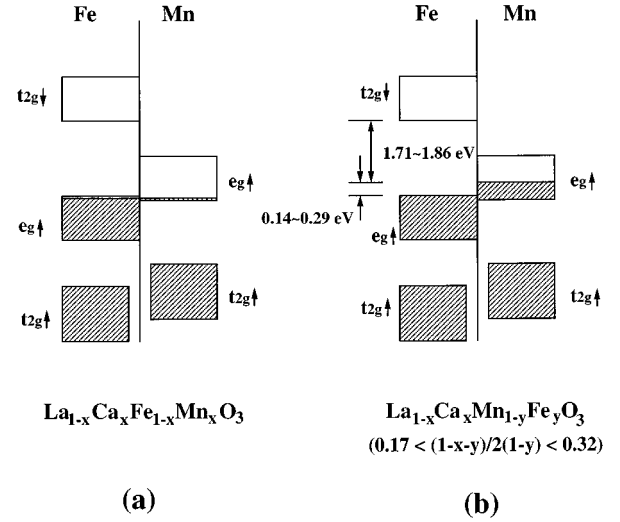


FIG. 4. Band structure of Fe and Mn in (a) $\text{La}_{1-x}\text{Ca}_x\text{Fe}_{1-x}\text{Mn}_x\text{O}_3$, where the bottom of the Mn $e_{g\uparrow}$ band lies slightly below the top of the Fe $e_{g\uparrow}$ band, and (b) $\text{La}_{1-x}\text{Ca}_x\text{Mn}_{1-y}\text{Fe}_y\text{O}_3$, where the Fe $e_{g\uparrow}$ band is completely filled and $(1-x-y)/2(1-y)$ of the Mn $e_{g\uparrow}$ band is filled.

ions are known to stay in the same spin state, due to the strong Hund's coupling. The vacant state with opposite spin lies higher in energy due to exchange interactions. Both occupied and unoccupied spin states are further split into t_{2g} and e_g orbitals by the octahedral crystal field. In increasing energy, these states are $t_{2g\uparrow}$, $e_{g\uparrow}$, $t_{2g\downarrow}$, and $e_{g\downarrow}$. The electronic configurations are $t_{2g\uparrow}^3 e_{g\uparrow}^2$ for Fe^{3+} , $t_{2g\uparrow}^3 e_{g\uparrow}^1$ for Fe^{4+} , and Mn^{3+} , and $t_{2g\uparrow}^3$ for Mn^{4+} , respectively. In a solid, these states form bands. For these ions, the $t_{2g\uparrow}$ bands are fully occupied, the $t_{2g\downarrow}$ and $e_{g\downarrow}$ bands are empty, and the $e_{g\uparrow}$ bands, which can accommodate a maximum of two electrons per ion, play a crucial role. In a mixed system of Fe and Mn, the widths and energies of their $e_{g\uparrow}$ bands dictate the electron distribution of the Fe and Mn ions.

Early study on the conductivity of $\text{La}_{0.85}\text{Ba}_{0.15}\text{Mn}_{1-x}\text{Fe}_x\text{O}_3$ by Jonker⁵ has shown that for $0 < x < 0.85$, Fe^{3+} , Mn^{3+} , and Mn^{4+} are present, and for $0.85 < x < 1.00$, Fe^{3+} , Fe^{4+} , and Mn^{4+} are present. The existence of Fe^{3+} , Mn^{3+} , and Mn^{4+} in the range of $0 < x < 0.85$, indicates that the Fe $e_{g\uparrow}$ band is full and the Mn $e_{g\uparrow}$ band is less than half-filled. For $0.85 < x < 1.00$, the existence of Mn^{4+} , Fe^{3+} , and Fe^{4+} means an empty Mn $e_{g\uparrow}$ band and a more than half-filled Fe $e_{g\uparrow}$ band. From this, it can be inferred that the bottom of the Mn $e_{g\uparrow}$ band should be at the same level as, or higher than, the top of the Fe $e_{g\uparrow}$ band. Thereby, the Fe $e_{g\uparrow}$ band remains completely filled as long as the Mn $e_{g\uparrow}$ band is partially filled.

Banks and Tashima⁸ have reached a similar conclusion by investigating the structural and conduction properties of a closely related system of $\text{La}_{1-x}\text{Ca}_x\text{Fe}_{1-x}\text{Mn}_x\text{O}_3$. They found that most Fe is present as Fe^{3+} , and at least 97% of the Mn exists as Mn^{4+} .⁸ They proposed the presence of a small amount (less than 3%) of Mn^{3+} and Fe^{4+} to account for the conductivity behavior in their samples. This conclusion agrees with the above band structure, where the top of the Fe $e_{g\uparrow}$ band is nearly at the bottom of the Mn $e_{g\uparrow}$ band, except

for a slight overlap (less than 3%) between the two, as shown in Fig. 4(a).

Our system of $\text{La}_{1-x}\text{Ca}_x\text{Mn}_{1-y}\text{Fe}_y\text{O}_3$ ($x=0.37$ and 0.53 , $y<0.20$) is expected to have a similar band structure as that of $\text{La}_{1-x}\text{Ca}_x\text{Fe}_{1-x}\text{Mn}_x\text{O}_3$. The nominal stoichiometry is $\text{La}^{3+}_{1-x}\text{Ca}^{2+}_x(\text{Mn}^{4+}_x\text{Mn}^{3+}_{1-x-y})\text{Fe}^{3+}_y\text{O}^{2-}_3$, for which both the Mn $t_{2g\uparrow}$ and Fe $t_{2g\uparrow}$ bands are filled. For the all important $e_{g\uparrow}$ bands, the Fe $e_{g\uparrow}$ band is completely filled, and $(1-x-y)/2(1-y)$ of the Mn $e_{g\uparrow}$ band is also filled. The latter filling factor is one half of the fraction of the Mn ions that are Mn^{3+} . The width of the Mn $e_{g\uparrow}$ band has been estimated to be about 1 eV.⁹ Assuming uniform filling for simplicity, and that the overlapped width of the Fe and Mn $e_{g\uparrow}$ bands is 3%, the Fermi surface would lie at $[(1-x-y)/2(1-y)-0.03]$ eV above the top of the Fe $e_{g\uparrow}$ band. Using the composition values of x and y for our series, the Fermi surface will lie 0.14 to 0.29 eV above the top of the Fe $e_{g\uparrow}$ band, as shown in Fig. 4(b). This energy diagram clearly illustrates that electron hopping between Fe and Mn is impeded by the lack of available states in the Fe $e_{g\uparrow}$ band. The only vacant states are in the Fe $t_{2g\downarrow}$ band, lying above the Fe $e_{g\uparrow}$ band, as shown in Fig. 4(b). However, Chainani, Mathew, and Sarma¹⁰ have shown that LaFeO_3 is an

insulator with an intrinsic gap of about 2.0 eV, which implies that the Fe $t_{2g\downarrow}$ band is located about 2 eV above the top of the Fe $e_{g\uparrow}$ band, or 1.71–1.86 eV above the Fermi surface for our system, as shown in Fig. 4(b). It is clear that electron hopping from Mn to Fe is energetically forbidden even at room temperature. Consequently, only the Mn $e_{g\uparrow}$ band is electronically active, where electron hopping can occur between Mn^{3+} and Mn^{4+} . Since Fe^{3+} replaces Mn^{3+} , doping with Fe causes a depletion of the $\text{Mn}^{3+}/\text{Mn}^{4+}$ ratio, the population of the hopping electrons, and the number of available hopping sites. Thus double exchange is suppressed, resulting in the reduction of ferromagnetism and metallic conduction.

In summary, we have observed suppression of ferromagnetism and conduction in both the FM and the AF phases of $\text{La}_{1-x}\text{Ca}_x\text{MnO}_3$ by doping Fe on the Mn sites. The usually dominant lattice effects have been bypassed due to the identical size of Mn^{3+} and Fe^{3+} . These results originate from the reduction of double exchange due to the depopulation of hopping electrons by the Fe doping.

This work was supported by NSF Grant No. DMR 95-01195.

¹R. von Helmolt *et al.*, Phys. Rev. Lett. **71**, 2331 (1993); S. Jin *et al.*, Science **264**, 413 (1994).

²P. Schiffer, A. P. Ramirez, W. Bao, and S.-W. Cheong, Phys. Rev. Lett. **75**, 3336 (1995).

³G.-Q. Gong, C. Canedy, G. Xiao, J. Z. Sun, A. Gupta, and W. J. Gallagher, Appl. Phys. Lett. **67**, 1783 (1995).

⁴C. Zener, Phys. Rev. **82**, 403 (1951); P.-G. de Gennes, *ibid.* **118**, 141 (1960).

⁵G. H. Jonker, Physica **20**, 1118 (1954).

⁶R. D. Shannon, Acta Crystallogr. A **32**, 751 (1976).

⁷H. L. Yakel, Jr., Acta Crystallogr. **8**, 394 (1955).

⁸E. Banks and N. Tashima, J. Appl. Phys. **41**, 1186 (1970).

⁹J. M. D. Coey, M. Viret, L. Ranno, and K. Ounadjela, Phys. Rev. Lett. **75**, 3910 (1995).

¹⁰A. Chainani, M. Mathew, and D. D. Sarma, Phys. Rev. B **48**, 14 818 (1993).